

Automat Control of the Aircrafts' Lateral Movement using the Dynamic Inversion

Mihai Lungu, Romulus Lungu, Lucian Grigorie

Abstract—The paper presents a new system for the automat control of the aircrafts' flight in lateral plane using the cinematic model and the dynamic inversion. Starting from the equations of the aircrafts' lateral movement, the authors use two axes systems and obtained a control law that cancels the lateral deviation of the flying objects from the runway line. This system makes the aircrafts' direction angle to follow the direction angle of the runway line. Simulations in Matlab/Simulink have been done for different aircrafts' initial points and direction angles. The inconvenience of this system is the long duration of the "transient regime". That is why this system can be used independently, but the results are not very good; thus, it can be a part (subsystem) of other systems. The main system that cancels the lateral deviation from the runway line is based on dynamic inversion and uses, as subsystem, the control system for the lateral movement using the cinematic model. Using complex Matlab/Simulink models, the authors obtained the time evolution of the direction angle and the time evolution of the aircraft lateral deviation with respect to the runway line, for different values of the initial direction angle and for different wind types. The system has a very good behavior for all initial direction angles and wind types.

Keywords—Direction angle, Dynamic inversion, Lateral deviation, Lateral movement

I. INTRODUCTION

ONE presents a system for the automat control of the aircrafts' lateral movement. This system eliminates or substantially reduces the lateral deviation of the aircraft with respect to the runway line's direction. This system uses an algorithm that elaborates the trajectory's command (yaw angular velocity $\dot{\psi}_c$, respectively the angle ψ_c) with respect to the tracing error; the imposed roll angle is $\varphi_c = 0$; that is why, the role of the ailerons is only to maintain the aircrafts' wing in horizontal plane. The system's control law is a non-linear one and controls the aircraft so that it follows a plan segment (for example, the runway) whatever the initial conditions (the coordinates and the aircraft's direction) are in the case of moderate wind. This law must be modified in the case of strong wind. For the testing of the control law, an aircraft cinematic model has been used.

M. Lungu is with the University of Craiova, Faculty of Electrical Engineering, Avionics Division, 107 Decebal Street, 200440 Craiova, Dolj, Romania, Email: Lma1312@yahoo.com, mlungu@elth.ucv.ro.

R. Lungu is with the University of Craiova, Faculty of Electrical Engineering, Avionics Division, 107 Decebal Street, 200440 Craiova, Dolj, Romania, Email: rlungu@elth.ucv.ro.

L. Grigorie is with the University of Craiova, Faculty of Electrical Engineering, Avionics Division, 107 Decebal Street, 200440 Craiova, Dolj, Romania, E-mail: lgrigorie@elth.ucv.ro, ltgrigorie@yahoo.com.

II. THE DETERMINATION OF THE CONTROL LAW

For the obtaining of the cinematic model [1], one considers that the aircraft flies in horizontal plane ($O\xi\eta$, $O\xi$ – tangent to the locus's parallel and East oriented, $O\eta$ – tangent to the locus's meridian and North oriented) and it is in a random position with respect to the imposed direction OT (in particular OT represents the direction of the runway line) – fig.1.

One chooses the axes Ox – same with OT and Oy – the perpendicular axis on Ox . The aircraft is initially in a point which has the coordinates (ξ_0, η_0) , respectively (x_0, y_0) .

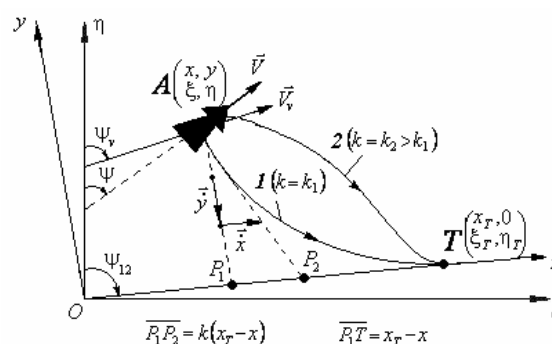


Fig.1 The trajectories and the parameters of the cinematic model

The aircraft flight velocity is \vec{V} and the reference direction for the aircraft to be oriented on is OT (T- the final point); the runway's direction is expressed by the mean of ψ_{12} angle. The point T has the coordinates $(x_T, 0)$ in the plane Oxy and (ξ_T, η_T) in the plane $O\xi\eta$.

The running distance, along Ox axis, till the moment when the lateral deviation y is zero, is $x_T - x$. If the trajectory of the aircraft in horizontal plane is the trajectory 1 from fig.1, then the tangent to this trajectory intersects the Ox axis in a point P_2 . The distance $\overline{P_1P_2}$ is $k(x_T - x)$, where k is a positive coefficient. Corresponding to the trajectory 1, the resultant $\vec{V}_{rez} = \vec{V} + \vec{V}_v$ (\vec{V}_v – the wind velocity) is the tangent to this trajectory and has the components \vec{x} and \vec{y} in a random point $A(x, y)$.

Between the coordinates of the two systems, one establishes the relationship [1]

$$\begin{bmatrix} \dot{x} \\ \dot{y} \end{bmatrix} = \underbrace{\begin{bmatrix} \sin \psi_{12} & \cos \psi_{12} \\ -\cos \psi_{12} & \sin \psi_{12} \end{bmatrix}}_{T_t} \begin{bmatrix} \dot{\xi} \\ \dot{\eta} \end{bmatrix}, \quad (1)$$

where T_t is the transformation matrix. Projecting \vec{V}_{rez} on the axes of the two coordinates systems, one obtains the equations

$$\begin{aligned} \dot{\xi} &= V_{\xi} + V_v \xi = V \sin \psi + V_v \sin \psi_v, \\ \dot{\eta} &= V_{\eta} + V_v \eta = V \cos \psi + V_v \cos \psi_v; \end{aligned} \quad (2)$$

$$\begin{aligned} \dot{x} &= V \cos(\psi_{12} - \psi) + V_v \cos(\psi_{12} - \psi_v), \\ \dot{y} &= V \sin(\psi_{12} - \psi) + V_v \sin(\psi_{12} - \psi_v), \end{aligned} \quad (3)$$

with $\psi = \psi(t)$. In the initial moment ($t = 0$), the aircraft has the known position $A(\xi_0, \eta_0)$, then, using (1), the coordinates (x_0, y_0) may be calculated, while the initial velocities are obtained with (3) with respect to the known variables V, V_v, ψ_{12} and with respect to the initial flight direction of the aircraft $\psi(0)$. For the calculus of the trajectory $y = f(x)$ one integrates equations (3) if the time evolution of ψ is known; $\dot{\psi}(t) = \omega_z(t)$ – the yaw angular velocity. If this is considered to be the command variable [1]

$$u(t) = \dot{\psi}(t) \quad (4)$$

for the system (3), with the state variables $x(t)$ and $y(t)$, then, if a control law $u(t)$ can be determined, it leads the aircraft on the desired trajectory. For the control law's obtaining, similar triangles for the velocities and coordinates are used. Thus, conform to fig.1, in every point $A(x, y)$, considering the modules of the angular velocities, one results the equation

$$\frac{\dot{x}}{k(x_T - x)} = \frac{\dot{y}}{y}, \quad (5)$$

similar with the one from [1].

For this equation, the error $E = k(x_T - x)\dot{y} - y\dot{x}$ is defined and it must tend to zero. That is why one chooses a proportional control law of form [1]

$$u(t) = \dot{\psi}(t) = k_R [k(x_T - x)\dot{y} - y\dot{x}], \quad k_R < 0; \quad (6)$$

conform to equation (1), $y_T = 0$ and

$$x_T = \xi_T \sin \psi_{12} + \eta_T \cos \psi_{12}. \quad (7)$$

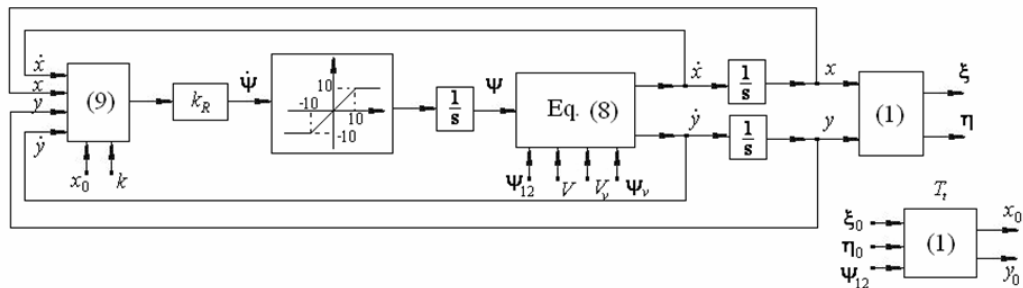


Fig.2 The block diagram for the modeling of the equations (8) and (9)

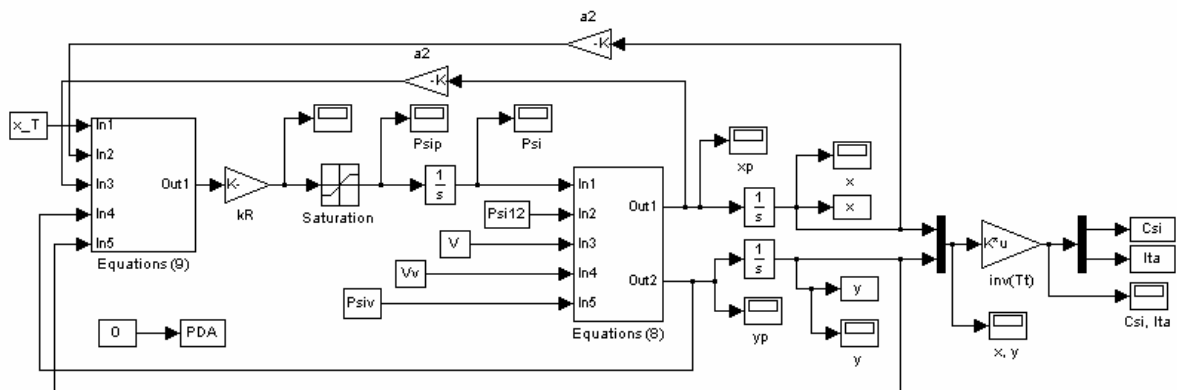


Fig.3 Matlab/Simulink model for the system from fig.2

Now, putting together the equations (3) and (6), a three order system is obtained (the state variables are x, y, ψ)

$$\begin{aligned} \dot{x} &= V \cos(\psi_{12} - \psi) + V_v \cos(\psi_{12} - \psi_v), \\ \dot{y} &= V \sin(\psi_{12} - \psi) + V_v \sin(\psi_{12} - \psi_v); \end{aligned} \quad (8)$$

$$\dot{\psi}(t) = k_R [k(x_T - x)\dot{y} - y\dot{x}], \quad (9)$$

The block diagram for the modeling of equations (8) and (9) is presented in fig.2. The nonlinearity with saturation has been used to assure the system's stability. In fig.3 the Matlab/Simulink model for the system from fig.2 is presented, while in fig.4 and fig.5 the authors present the Matlab/Simulink models of the two subsystems "Equations (8)" and "Equations 9" of the model from fig.3.

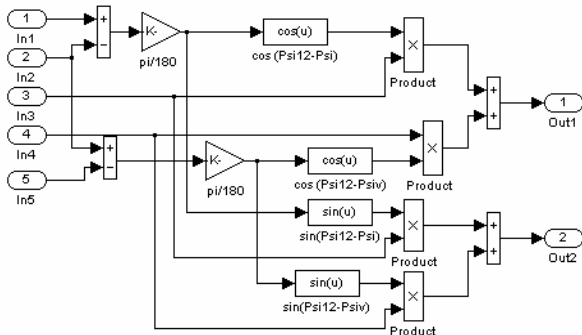


Fig.4 Matlab/Simulink model for the subsystem "Equations (8)"

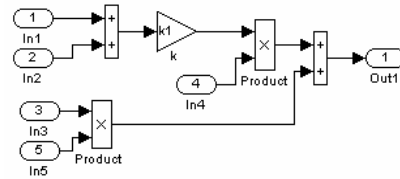


Fig.5 Matlab/Simulink model for the subsystem "Equations (9)"

The simulation of the system from fig.2 is made for different cases: without wind or with wind (with different velocities and directions).

In fig.6.a one represents the trajectories $\eta(\xi)$, starting from a point $A_0(\xi_0, \eta_0) \equiv A_0(x_0, y_0)$, for $\psi = 30 \text{ deg}$, $\psi_{12} = 60 \text{ deg}$ and k - variable (0.4, 0.5, 0.6, 0.7, 0.8, 0.9); $V = 80 \text{ m/s}$, $V_v = 0 \text{ m/s}$. The coordinates (x_0, y_0) are calculated with (1) with respect to (ξ_0, η_0) and ψ_{12} ; one considers $\xi_0 = 1000 \text{ m}$, $\eta_0 = 2000 \text{ m}$; the coordinates of the point T are $\xi_T = 2000 \text{ m}$, $\eta_T = \xi_0 / \tan(\psi_{12})$. Same trajectories are represented in fig.7.a (for the same values, but for $V_v = 15 \text{ m/s}$ and $\psi_v = 45 \text{ deg}$) and in fig.8.a (for the same values, but for $V_v = 10 \text{ m/s}$ and $\psi_v = 120 \text{ deg}$).

In fig.6.b one represents the trajectories $\eta(\xi)$, starting from a point $A_0(\xi_0, \eta_0) \equiv A_0(x_0, y_0)$, for ψ - variable angle and $k = 0.4$; the other values are the values used in fig.6.a; in fig.7.b the authors obtained the trajectories $\eta(\xi)$, for the same values, but for $V_v = 15 \text{ m/s}$ and $\psi_v = 45 \text{ deg}$;

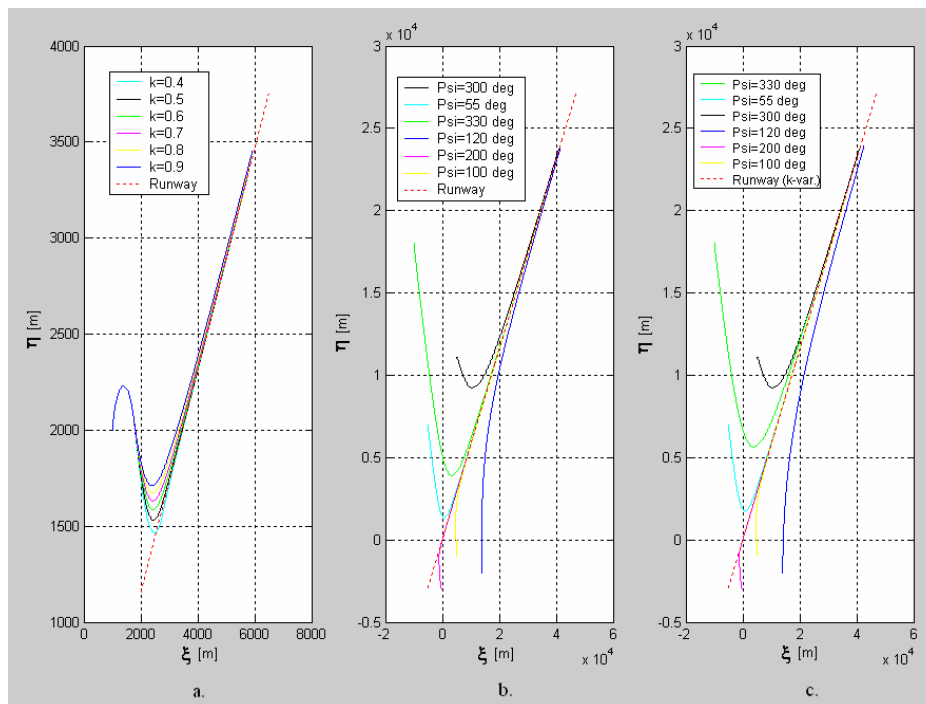


Fig. 6 The trajectories $\eta(\xi)$ of the aircraft for $V_v = 0 \text{ m/s}$, $\psi_v = 0 \text{ deg}$

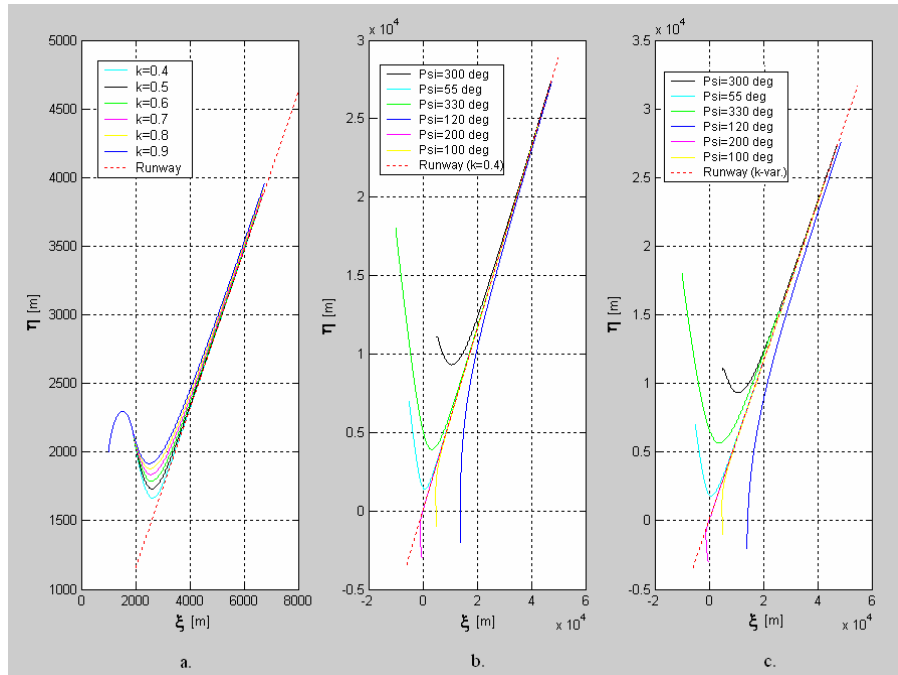


Fig. 7 The trajectories $\eta(\xi)$ of the aircraft for $V_v = 15 \text{ m/s}$, $\psi_v = 45 \text{ deg}$

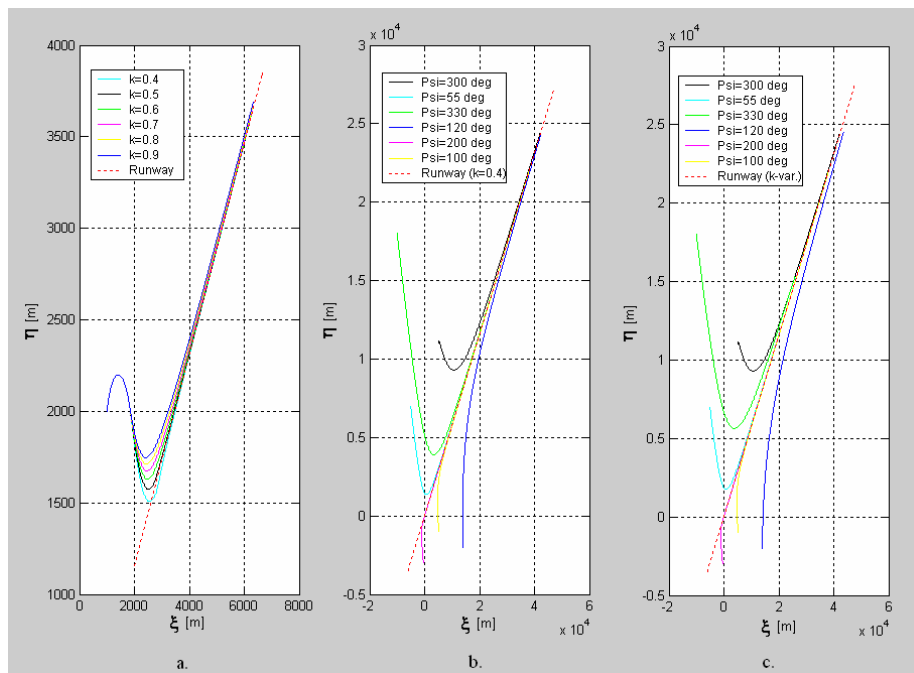


Fig. 8 The trajectories $\eta(\xi)$ of the aircraft for $V_v = 10 \text{ m/s}$, $\psi_v = 120 \text{ deg}$

similarly, one obtained the characteristics from fig.8.b ($V_v = 10 \text{ m/s}$ and $\psi_v = 120 \text{ deg}$).

In fig.6.c one represents the trajectories $\eta(\xi)$, for different points $A_0(\xi_0, \eta_0) \equiv A_0(x_0, y_0)$, ψ - variable angle and k - variable coefficient; similarly, in fig.7.c and fig.8.c the characteristics of the aircraft (for $V_v = 15 \text{ m/s}$ and $\psi_v = 45 \text{ deg}$, respectively $V_v = 10 \text{ m/s}$ and $\psi_v = 120 \text{ deg}$) are presented.

As one can see, in all cases, the aircraft tends to follow the runway line. The inconvenience of this system is the long duration of the “transient regime”. Whatever the aircraft’s initial point and its initial direction are, the aircraft follows the direction of the runway line ($\psi \rightarrow \psi_{12}$). Because of the long duration of the “transient regime” this system can not be used independently; it can be a part (subsystem) of other systems. For example, in this paper, it will be the subsystem of the system from fig.9.

III. EQUATIONS OF THE AIRCRAFT' LATERAL MOVEMENT

Before the obtaining of the aircrafts' dynamic inversion model (lateral movement), the authors have to present the model of the lateral movement for the aircraft chosen for simulations (Charlie-1 aircraft) [2].

The main sensors that are used on aircrafts are: three accelerometers (for the measurement of the accelerations a_x, a_y, a_z , which, by integrating, lead to velocities V_x, V_y, V_z) and three gyrometers (for the measurement of the angular velocities $\omega_x, \omega_y, \omega_z$), connected in an inertial navigation system (INS), sensors for static and dynamic pressure (the first for the determination of the barometric altitude and the both sensors for the determination of the flight velocity), a radio-altimeter or other system for the measurement of the aircraft's height with respect to the ground and so on [3], [4]. All these sensors are used for the measurement of the lateral movement's variables.

The equations of the aircraft's lateral movement are [5]

$$\begin{aligned} \Delta \dot{V}_y &= Y_v \Delta V_y - V_{x0} \Delta \omega_z + g \cos \theta_0 \Delta \varphi + Y_{\delta_d} \Delta \delta_d, \\ \Delta \dot{\omega}_x &= L'_v \Delta V_y + L'_p \Delta \omega_x + L'_r \Delta \omega_z + L'_{\delta_e} \Delta \delta_e + L'_{\delta_d} \Delta \delta_d, \\ \Delta \dot{\omega}_z &= N'_v \Delta V_y + N'_p \Delta \omega_x + N'_r \Delta \omega_z + N'_{\delta_e} \Delta \delta_e + N'_{\delta_d} \Delta \delta_d, \\ \Delta \dot{\varphi} &= \Delta \omega_x + \operatorname{tg} \theta_0 \cdot \Delta \omega_z, \\ \Delta \dot{\psi} &= \sec \theta_0 \cdot \Delta \omega_z, \end{aligned} \quad (10)$$

where δ_e, δ_d – the deflections of the ailerons and of the rudder, φ, ψ – the roll and the direction angles, $\omega_x = \dot{\varphi}$ – the roll angular velocity, $\omega_z = \dot{\psi}$ – the yaw angular velocity V_y – the component of the velocity vector \vec{V} with respect to the lateral axis of the aircraft (Oy).

Ignoring, by notation, the symbol Δ , the state equation that describes the lateral movement of the aircraft is

$$\dot{\mathbf{x}} = \mathbf{Ax} + \mathbf{Bu}, \quad (11)$$

with the state vector $\mathbf{x} = [V_y \ \omega_x \ \omega_z \ \varphi \ \psi]^T$, the command vector $\mathbf{u} = [\delta_e \ \delta_d]^T$, and the matrices \mathbf{A} and \mathbf{B} of forms

$$\mathbf{A} = \begin{bmatrix} a_{11} & a_{12} & a_{13} & a_{14} & 0 \\ a_{21} & a_{22} & a_{23} & a_{24} & 0 \\ a_{31} & a_{32} & a_{33} & a_{34} & 0 \\ 0 & 1 & \tan(\theta_0) & 0 & 0 \\ 0 & 0 & \sec(\theta_0) & 0 & 0 \end{bmatrix} = \begin{bmatrix} Y_v & 0 & -V_{x0} & g \cos \theta_0 & 0 \\ L'_v & L'_p & L'_r & 0 & 0 \\ N'_v & N'_p & N'_r & 0 & 0 \\ 0 & 1 & \tan(\theta_0) & 0 & 0 \\ 0 & 0 & \sec(\theta_0) & 0 & 0 \end{bmatrix}, \quad (12)$$

$$\mathbf{B} = \begin{bmatrix} b_{11} & b_{12} \\ b_{21} & b_{22} \\ b_{31} & b_{32} \\ b_{41} & b_{42} \\ b_{51} & b_{52} \end{bmatrix} = \begin{bmatrix} 0 & Y_{\delta_d} \\ L'_{\delta_e} & L'_{\delta_d} \\ N'_{\delta_e} & N'_{\delta_d} \\ 0 & 0 \\ 0 & 0 \end{bmatrix}.$$

The elements of the above matrices are calculated with

respect to the stability derivatives, using the equations [5]

$$\begin{aligned} I_A &= \frac{J_{xz}}{J_{xx}}, I_B = \frac{J_{xz}}{J_{zz}}, I' = 1 - L_p - I_A I_B - N_p I_{AB}, \\ L'_v &= \frac{L_v + I_A N_v}{I'}, L'_p = \frac{L_p + I_A N_p}{I'}, L'_r = \frac{L_r + I_A N_r}{I'}, \\ N'_v &= \frac{L_v I_B (+ N_p) + N_v}{I'}, N'_p = \frac{L_p I_B + N_p}{I'}, N'_r = \frac{L_r I_B + N_r}{I'}, \\ L'_{\delta_e} &= \frac{L_{\delta_e} + I_A N_{\delta_e}}{1 - I_A I_B}, L'_{\delta_d} = \frac{L_{\delta_d} + I_A N_{\delta_d}}{1 - I_A I_B}, \\ N'_{\delta_e} &= \frac{L_{\delta_e} I_B + N_{\delta_e}}{I'}, N'_{\delta_d} = \frac{L_{\delta_d} I_B + N_{\delta_d}}{I'}. \end{aligned} \quad (13)$$

For the Charlie-1 aircraft, the coefficients that interfere in equations (12) and (13) are

$$\begin{aligned} V_0 &= 67 [m/s], Y_v = -0.089 [\text{deg}/m \cdot s], \\ L'_v &= -1.33 [\text{deg}/m \cdot s], L'_p = -0.98 [1/s], \\ L'_r &= 0.33 [1/s], N'_v = 0.17 [\text{deg}/m \cdot s], \\ N'_p &= -0.17 [1/s], N'_r = -0.217 [1/s], \\ Y_{\delta_d} &= 1 [m/\text{deg} \cdot s^2], \\ L'_{\delta_e} &= 0.23 [1/s^2], L'_{\delta_d} = 0.06 [1/s^2], \\ N'_{\delta_e} &= 0.026 [1/s^2], N'_{\delta_d} = -0.15 [1/s^2]. \end{aligned} \quad (14)$$

Thus, the dynamics of the lateral movement is described by the state equation (11) and by the matrices

$$\mathbf{A} = \begin{bmatrix} -0.089 & 0 & -67 & 9.81 & 0 \\ -1.33 & -0.98 & 0.33 & 0 & 0 \\ 0.17 & -0.17 & -0.217 & 0 & 0 \\ 0 & 1 & 0 & 0 & 0 \\ 0 & 0 & 1 & 0 & 0 \end{bmatrix}, \mathbf{B} = \begin{bmatrix} 0 & 1 \\ 0.23 & 0.06 \\ 0.026 & -0.15 \\ 0 & 0 \\ 0 & 0 \end{bmatrix}. \quad (15)$$

IV. INVERSION OF THE AIRCRAFTS' DYNAMIC MODEL

A lot of flight automat control structures are based on the dynamic inversion principle [6], [7], [8]. Thus, the linear dynamic model of the aircrafts' rotation movement is described by equation

$$\dot{\omega} = A_\omega \omega + A_v V + B \delta_c, \quad (16)$$

with $\omega = [\omega_x \ \omega_y \ \omega_z]^T$ – the vector containing the angular velocities of the aircraft, $V = [V_x \ V_y \ V_z]^T$ – the aircraft's translations velocities vector (with its components), $\delta_c = [\delta_p \ \delta_e \ \delta_d]^T$ – the vector containing the command deflection of the elevator, ailerons and rudder, A_v – (3×3) matrix that defines the rotations and the translations of the aircraft, B – (3×3) inversable input matrix. By dynamic inversion, the control law

$$\delta_c = B^{-1}(\dot{\omega} - A_\omega \omega - A_v V) \quad (17)$$

is obtained. From (10) one extracts the second and the third differential equations

$$\dot{\omega}_x = a_{21}V_y + a_{22}\omega_x + a_{23}\omega_z + a_{24}\varphi + b_{21}\delta_e + b_{22}\delta_d, \quad (18)$$

$$\dot{\omega}_z = a_{31}V_y + a_{32}\omega_x + a_{33}\omega_z + a_{34}\varphi + b_{31}\delta_e + b_{32}\delta_d. \quad (19)$$

This model may be expressed by the equation

$$\begin{bmatrix} \dot{\omega}_x \\ \dot{\omega}_z \end{bmatrix} = \begin{bmatrix} a_{21} \\ a_{31} \end{bmatrix} V_y + \begin{bmatrix} a_{22} & a_{23} \\ a_{32} & a_{33} \end{bmatrix} \begin{bmatrix} \omega_x \\ \omega_z \end{bmatrix} + \begin{bmatrix} a_{24} \\ a_{34} \end{bmatrix} \varphi + \begin{bmatrix} b_{21} & b_{22} \\ b_{31} & b_{32} \end{bmatrix} \begin{bmatrix} \delta_e \\ \delta_d \end{bmatrix}. \quad (20)$$

From the above equation, the lateral movement's inverse model is obtained

$$\begin{bmatrix} \delta_e \\ \delta_d \end{bmatrix} = \begin{bmatrix} b_{21} & b_{22} \\ b_{31} & b_{32} \end{bmatrix}^{-1} \left\{ \begin{bmatrix} \dot{\omega}_{xc} \\ \dot{\omega}_{zc} \end{bmatrix} - \begin{bmatrix} a_{21} \\ a_{31} \end{bmatrix} V_y - \begin{bmatrix} a_{22} & a_{23} \\ a_{32} & a_{33} \end{bmatrix} \begin{bmatrix} \omega_x \\ \omega_z \end{bmatrix} - \begin{bmatrix} a_{24} \\ a_{34} \end{bmatrix} \varphi \right\}; \quad (21)$$

ω_{xc} and ω_{zc} are the calculated angular velocities; in many cases $a_{24} = a_{34} = 0$ and the equation (21) has the form (17).

For the obtaining of the command inputs of the aircrafts flight' automat control subsystems, one uses two reference models (command filters – law pass filters).

The subsystem's order, represented by each command filter, is equal with the relative degree of the subsystem's model whose output is the state variable commanded by the respective filter's output. Thus, for the command of the roll angle (φ) and of the direction angle (ψ), two identical filters have been used; the filters have the transfer functions

$$\frac{\bar{\varphi}(s)}{\varphi_c(s)} = \frac{\omega_n^2}{s^2 + 2\xi\omega_n s + \omega_n^2}, \quad (22)$$

$$\frac{\bar{\psi}(s)}{\psi_c(s)} = \frac{\omega_n^2}{s^2 + 2\xi\omega_n s + \omega_n^2},$$

with ω_n – the frequency (natural pulsation) and ξ – the damping coefficient. The filter for the roll angle (φ) provides the output signals $\bar{\varphi}$, $\dot{\bar{\varphi}}$, $\ddot{\bar{\varphi}}$ and, by the integration of $\bar{\varphi}$, $\int \bar{\varphi} dt$ may also be obtained. Same signals are used for the direction angle (ψ). Using these signals, the components of the angular accelerations $\ddot{\varphi}_c$ and $\ddot{\psi}_c$ are calculated [9]

$$\ddot{\varphi}_c = \ddot{\bar{\varphi}} + k_p^{\varphi}(\bar{\varphi} - \varphi) + k_e^{\varphi}(\dot{\bar{\varphi}} - \dot{\varphi}) + k_{ei}^{\varphi} \int (\bar{\varphi} - \varphi) dt,$$

$$\ddot{\psi}_c = \ddot{\bar{\psi}} + k_p^{\psi}(\bar{\psi} - \psi) + k_e^{\psi}(\dot{\bar{\psi}} - \dot{\psi}) + k_{ei}^{\psi} \int (\bar{\psi} - \psi) dt. \quad (23)$$

For the obtaining of the imposed angular accelerations ($\dot{\omega}_{xc}$, $\dot{\omega}_{zc}$), the authors use the two command filters and two

proportional – derivative controller ($k_{ei}^{\varphi} = k_{di}^{\psi} = 0$) [10], [11], [12], [13]; the derivative components stabilize the system with angular velocities steady errors equal with zero, while the angular accelerations $\ddot{\bar{\varphi}}$, $\ddot{\bar{\psi}}$ lead to faster time responses.

The expressions of the imposed angular accelerations $\dot{\omega}_{xc}$, $\dot{\omega}_{zc}$ are obtained by the derivative of the equations [5]

$$\omega_x = \dot{\varphi} - \dot{\psi} \sin \theta,$$

$$\omega_z = -\dot{\theta} \sin \varphi + \dot{\psi} \cos \theta \cos \varphi, \quad (24)$$

where $\dot{\omega}_x$, $\dot{\omega}_z$ and $\ddot{\varphi}$, $\ddot{\psi}$ are replaced by $\dot{\omega}_{xc}$, $\dot{\omega}_{zc}$ and $\ddot{\varphi}_c$, $\ddot{\psi}_c$; it yields (θ – the pitch angle of the aircraft)

$$\dot{\omega}_{xc} = \ddot{\varphi}_c - \ddot{\psi}_c \sin \theta - \dot{\psi} \dot{\theta} \cos \theta,$$

$$\dot{\omega}_{zc} = -\ddot{\theta}_c \sin \varphi - \dot{\theta} \dot{\varphi} \cos \varphi + \ddot{\psi}_c \cos \theta \sin \varphi - \dot{\psi} (\dot{\theta} \sin \theta \cos \varphi + \dot{\varphi} \cos \theta \sin \varphi). \quad (25)$$

Angular velocities $\dot{\varphi}_c$, $\dot{\psi}_c$ from equations (18) and (19) are obtained using equation (23). For the aircrafts' lateral movement

$$\dot{\omega}_{xc} = \dot{\varphi}_c,$$

$$\dot{\omega}_{zc} = \dot{\psi}_c. \quad (26)$$

V. AUTOMAT CONTROL OF THE LATERAL MOVEMENT BASED ON DYNAMIC INVERSION

The system for the automat control of the aircrafts in lateral plane, based on dynamic inversion, is presented in fig.9. This new system may be used, with good results, to the automat control of the aircrafts in the landing process.

The two command filters have the transfer functions 22 with $\omega_n = 0.8 \text{ rad} / \text{s}$, $\xi = 0.3$.

The constants of the two controllers have been chosen by the paper's authors

$$k_d^{\psi} = k_e^{\varphi} = 2.2 \cdot 10^{-3} [1 / \text{s}^2],$$

$$k_d^{\varphi} = k_e^{\psi} = 4 \cdot 10^{-2} [1 / \text{s}] \quad (27)$$

and the time constants of the servo-rudder and servo-ailerons are

$$T_d = T_e = 0.7 \text{ s}. \quad (28)$$

In fig.10, the authors present the Matlab/Simulink model for the block diagram from fig.9. This Matlab/Simulink model has 4 subsystems: "Command filter Psi" – fig.11, "Command filter Fi" – fig.11, "Subsystem – control law forming" – fig.3 and "Equations (21)" – fig.12.

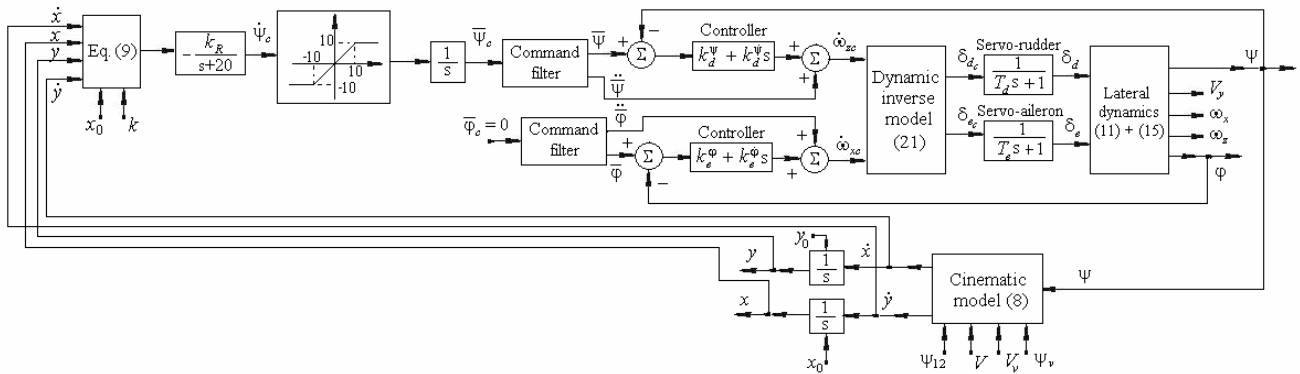


Fig. 9 The system for the automat control of the aircrafts in lateral plane, based on dynamic inversion using the cinematic model

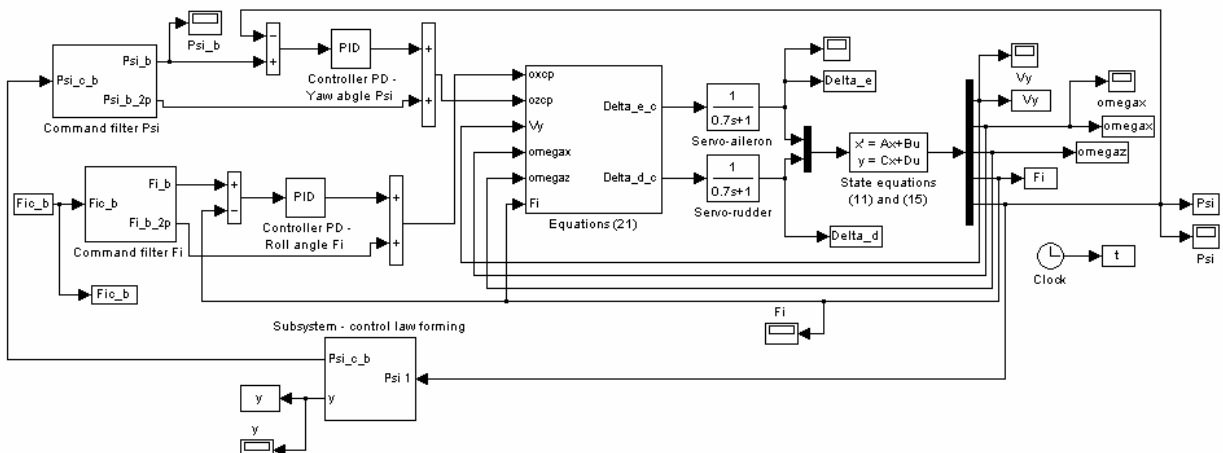


Fig. 10 Matlab/Simulink model for the system from fig.9

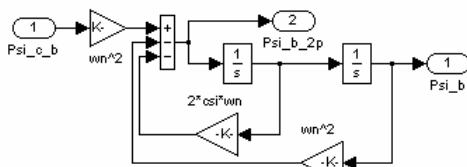


Fig.11 Matlab/Simulink model for the subsystems
 "Command filter Psi" and "Command filter Fi"

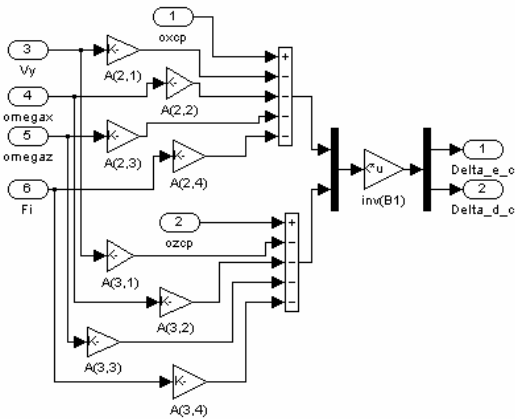


Fig.12 Matlab/Simulink model for the subsystem "Equations (21)"

By the simulation of the Matlab/Simulink model from fig.10 the authors obtained the time characteristics from fig.13. Here, four cases have been studied:

- $V_v = 0 \text{ m/s}, \psi_v = 0 \text{ deg}$ (no wind);
- $V_v = 15 \text{ m/s}, \psi_v = 45 \text{ deg}$;
- $V_v = 10 \text{ m/s}, \psi_v = 120 \text{ deg}$;
- $V_v = 5 \text{ m/s}, \psi_v = \psi_{12} = 60 \text{ deg}$.

For each case the authors present the time evolution of the direction angle ψ and the time evolution of the aircraft lateral deviation y with respect to the runway line.

As one can see, for all 4 cases, the direction angle tends to the desired value $\psi_{12} = 60 \text{ deg}$.

The initial value of the direction angle ψ varies (30 deg, 80 deg., 120 deg. and 200 deg.). Whatever the initial value of the direction angle is, the system responds very good and cancels the lateral deviation of the aircraft from the runway line. The system has a very good behavior for all initial direction angles.

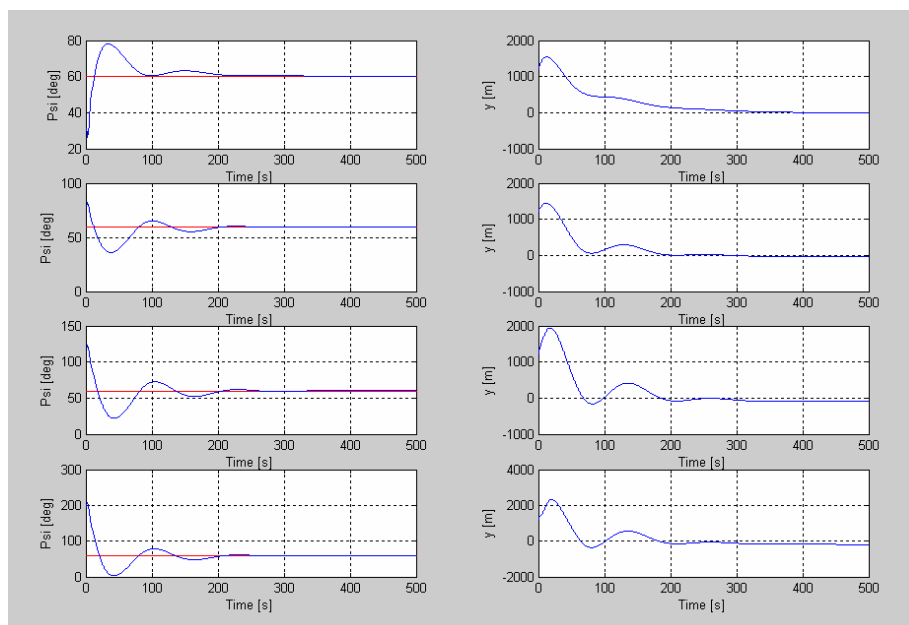


Fig.13 Time variation of the direction angle ψ and of the lateral deviation y with respect to the runway line

VI. CONCLUSION

The paper presents a new system for the automat control of the aircrafts' flight in lateral plane using the cinematic model and the dynamic inversion. This new system (automat pilot), presented in this paper, may be used, with good results, to the automat control of the aircrafts in the landing process. Its main subsystem is a system that makes the aircrafts' direction angle to follow the direction angle of the runway line. For this subsystem, Matlab simulations have been done for different aircraft's initial points and direction angles. Because of the long transient regime that characterizes this subsystem, it is better to use it as a part of other systems. One of these systems is presented in this paper - the system for the automat control of the aircrafts in lateral plane, based on dynamic inversion using the cinematic model (fig.9).

Using complex Matlab/Simulink models, the authors obtained the time evolution of the direction angle and the time evolution of the aircraft lateral deviation with respect to the runway line, for different values of the initial direction angle and for different wind types. The system has a very good behavior (it cancels the lateral deviation from the runway line) for all initial direction angles and wind types.

ACKNOWLEDGMENT

This work was supported by CNCSIS-UEFISCSU, project PN II-RU "High-precision strap-down inertial navigators, based on the connection and adaptive integration of the nano and micro inertial sensors in low cost networks, with a high degree of redundancy", code102/2010.

REFERENCES

- [1] M. Niculescu, "Lateral Track control Law for Aerosonde UAV". AIAA no. 2001-0016, pp. 1-11, 2001, 39th AIAA Aerospace Science Meeting and Exhibit, 8-11 January 2001, Reno.
- [2] Mc.L. Donald, *Automatic Flight Control Systems*. Prentice Hall Publisher, 1990, 593 pp.
- [3] V. Riczny, J. Mikulec, "Measuring flying object velocity with CCD sensors". *IEEE Aerospace and Electronic Systems Magazine*, vol.9, Issue 6, pp. 3-6, June 1994.
- [4] B. Gollomp, "The angle of attack". *IEEE Instrumentation & Measurement Magazine*, vol.4, Issue 1, pp. 57-58, 2001.
- [5] M. Lungu, *Sisteme de conducere a zborului*. Sitech Publisher, 2008.
- [6] Mackunis, P.M. Patre, M.K. Kaise, W.E. Dixon, "Asymptotic Tracking for Aircraft via Robust and Adaptive Dynamic Inversion Methods", *IEEE Transactions on Control Systems and Technology*, vol. 18, no.6, 2010.
- [7] N.A. Denison, *Automated Carrier Landing of an Unmanned Combat Aerial Vehicle Using Dynamic Inversion*, Master's thesis, June 2007.
- [8] H.B. Chen, S.G. Zhang, "Robust dynamic inversion flight control law design", 2nd International Symposium on Systems and Control in Aerospace and Astronautics, Shenzhen, December 2008.
- [9] A.J. Calise, R.T. Rysdyk, "Adaptive Model Inversion Flight Control for Tiltrotor Aircraft", *AIAA Guidance, Navigation and Control*, vol. 22, pp. 402-407, 1999.
- [10] C. Huang, Q. Shao, P. Jin, Z. Zhu, P. Luoyang, "Pitch Attitude Controller Design and Simulation for a Small Unmanned Aerial Vehicle". International Conference on Intelligent Human-Machine Systems and Cybernetics, IHMSC '09, Hangzhou, Zhejiang, 26-27 Aug. 2009, pp. 58-61.
- [11] S. Santos, N. Oliveira, "Test platform to pitch angle using hardware in loop". 39th IEEE Frontiers in Education Conference, FIE '09, San Antonio, 18-21 Oct. 2009, pp. 1-5.
- [12] A.A. Pashilkar, N. Sundararajan, P.A. Saratchandran, "Fault-Tolerant Neural Aided Controller for Aircraft Auto-Landing". *Aerospace Science and Technology*, vol.10, Issue 1. 2006, pp. 49-61.
- [13] V. Kargin, *Design of An Autonomous Landing Control Algorithm for A Fixed Wing UAV*. MS Thesys, Middle East Technical University, Ankara, Turkey, 2007.